Medical Image Analysis 15 (2011) 670–679

Contents lists available at ScienceDirect

Medical Image Analysis

journal homepage: www.elsevier.com/locate/media

Efficient MR image reconstruction for compressed MR imaging

Junzhou Huang *, Shaoting Zhang, Dimitris Metaxas

Department of Computer Science, 110 Frelinghuysen Road Piscataway, NJ 08854-8019, USA

ARTICLE INFO

Article history:
Available online 24 June 2011

Keywords:
Convex optimization
Compressive sensing
MR image reconstruction

ABSTRACT

In this paper, we propose an efficient algorithm for MR image reconstruction. The algorithm minimizes a linear combination of three terms corresponding to a least square data fitting, total variation (TV) and $L1$ norm regularization. This has been shown to be very powerful for the MR image reconstruction. First, we decompose the original problem into $L1$ and TV norm regularization subproblems respectively. Then, these two subproblems are efficiently solved by existing techniques. Finally, the reconstructed image is obtained from the weighted average of solutions from two subproblems in an iterative framework. We compare the proposed algorithm with previous methods in term of the reconstruction accuracy and computation complexity. Numerous experiments demonstrate the superior performance of the proposed algorithm for compressed MR image reconstruction.

1. Introduction

Magnetic Resonance (MR) imaging has been widely used in medical diagnosis because of its non-invasive manner and excellent depiction of soft tissue changes. Recent developments in compressive sensing theory (Candes et al., 2006; Donoho, 2006) show that it is possible to accurately reconstruct the Magnetic Resonance (MR) images from highly undersampled K-space data and therefore significantly reduce the scanning duration.

Suppose x is a MR image and R is a partial Fourier transform, the sampling measurement b of x in K-space is defined as $b = Rx$. The compressed MR image reconstruction problem is to reconstruct x given the measurement b and the sampling matrix R. Motivated by the compressive sensing theory, Lustig et al. (Lustig et al., 2007) proposed their pioneering work for the MR image reconstruction. Their method can effectively reconstruct MR images with only 20% sampling. The improved results were obtained by having both a wavelet transform and a discrete gradient in the objective, which is formulated as follows:

$$\hat{x} = \arg\min_x \left\{ \frac{1}{2}\|Rx - b\|^2 + \alpha\|x\|_{TV} + \beta\|\Phi x\|_1 \right\} \quad (1)$$

where α and β are two positive parameters, b is the undersampled measurements of K-space data, R is a partial Fourier transform and Φ is a wavelet transform. It is based on the fact that the piecewise smooth MR images of organs can be sparsely represented by the wavelet basis and should have small total variations. The TV was defined discretely as $\|x\|_{TV} = \sum_i \sum_j ((\nabla_1 x_{ij})^2 + (\nabla_2 x_{ij})^2)$ where ∇_1 and ∇_2 denote the forward finite difference operators on the first and second coordinates, respectively. Since both $L1$ and TV norm regularization terms are nonsmooth, this problem is very difficult to solve. The conjugate gradient (CG) (Lustig et al., 2007) and PDE (He et al., 2006) methods were used to attack it. However, they are very slow and impractical for real MR images. Computation became the bottleneck that prevented this good model (1) from being used in practical MR image reconstruction. Therefore, the key problem in compressed MR image reconstruction is thus to develop efficient algorithms to solve problem (1) with nearly optimal reconstruction accuracy.

Other methods tried to reconstruct compressed MR images by performing L_p-quasinorm ($p < 1$) regularization optimization (Ye et al., 2007; Chartrand, 2007; Chartrand, 2009). Although they may achieve a little bit of higher compression ratio, these nonconvex methods do not always give global minima and are also relatively slow. Trzasko et al. (Trzasko et al., 2009) used the homotopic nonconvex L_0-minimization to reconstruct MR images. They created a gradual nonconvex objective function which may allow global convergence with designed parameters. It was faster than those L_p-quasinorm regularization methods. However, it still needed 1–3 min to obtain reconstructions of 256×256 images in MATLAB on a 3 GHz desktop computer. Recently, two fast methods were proposed to directly solve (1). In (Ma et al., 2008), Ma et al. proposed an operator-splitting algorithm (TVCMRI) to solve the MR image reconstruction problem. In Yang et al. (2010), a variable splitting method (RecPF) was proposed to solve the MR image reconstruction problem. Both of them can replace iterative linear solvers with Fourier domain computations, which can gain substantial time savings. In MATLAB on a 3 GHz desktop computer, they can be used to obtain good reconstructions of 256×256 images in ten seconds or less. They are two of the fastest MR image reconstruction methods so far.

* Corresponding author.
E-mail address: jzhuang@cs.rutgers.edu (J. Huang).

1361-8415/$ - see front matter © 2011 Elsevier B.V. All rights reserved.
doi:10.1016/j.media.2011.06.001

Model (1) can be interpreted as a special case of general optimization problems consisting of a loss function and convex functions as priors. Two classes of algorithms to solve this generalized problem are operator-splitting algorithms and variable-splitting algorithms. Operator-splitting algorithms search for an x that makes the sum of the corresponding maximal-monotone operators equal to zero. These algorithms widely use the Forward–Backward schemes (Gabay, 1983; Combettes and Wajs, 2008; Tseng, 2000), Douglas-Rachford splitting schemes (Spingarn, 1983) and projective splitting schemes (Eckstein and Svaiter, 2009). The Iterative Shrinkage-Thresholding Algorithm (ISTA) and Fast ISTA (FISTA) (Beck and Teboulle, 2009b) are two well known operator-splitting algorithms. They have been successfully used in signal processing (Beck and Teboulle, 2009b; Beck and Teboulle, 2009a) and multitask learning (Ji and Ye, 2009). Variable splitting algorithms, on the other hand, are based on combinations of alternating direction methods (ADM) under an augmented Lagrangian framework. It is firstly used to solve the PDE problem in Gabay and Mercier (1976), Glowinski and Le Tallec (1989). Tseng and He et al. extended it to solve variational inequality problems (Tseng, 1991; He et al., 2002). Wang et al. (2008) showed that the ADMs are very efficient for solving TV regularization problems. They also outperform previous interior-point methods on some structured SDP problems (Malick et al., 2009). Two variable-splitting algorithms, namely the Multiple Splitting Algorithm (MSA) and Fast MSA (FaMSA), have been recently proposed to efficiently solve (1), while all convex functions are assumed to be smooth (Goldfarb and Ma, 2009).

However, all these above-mentioned algorithms can not efficiently solve (1) with provable convergence complexity. Moreover, none of them can provide the complexity bounds of iterations for their problems, except ISTA/FISTA in Beck and Teboulle (2009b) and MSA/FaMSA in Goldfarb and Ma (2009). Both ISTA and MSA are first order methods. Their complexity bounds are $O(1/\epsilon)$ for ϵ-optimal solutions. Their fast versions, FISTA and FaMSA, have complexity bounds $O(1/\sqrt{\epsilon})$, which are inspired by the seminal results of Nesterov and are optimal according to the conclusions of Nesterov (1983, 2007). However, both ISTA and FISTA are designed for simpler regularization problems and can not be applied efficiently to the composite regularization problem (1) using both $L1$ and TV norm. While the MSA/FaMSA assume that all convex functions are smooth, it makes them unable to directly solve the problem (1) as we have to smooth the nonsmooth function first before applying them. Since the smooth parameters are related to ϵ, the FaMSA with complexity bound $O(1/\sqrt{\epsilon})$ requires $O(1/\epsilon)$ iterations to compute an ϵ-optimal solution, which means that it is not optimal for this problem. Section 2.1 will further introduce the related algorithms in details.

In this paper, we propose a new optimization algorithm for MR image reconstruction method. It is based on the combination of both variable and operator splitting techniques. We decompose the hard composite regularization problem (1) into two simpler regularization subproblems by: (1) splitting variable x into two variables $\{x_i\}_{i=1,2}$; (2) performing operator splitting to minimize total variation regularization and L1 norm regularization subproblems over $\{x_i\}_{i=1,2}$ respectively and (3) obtaining the solution x by linear combination of $\{x_i\}_{i=1,2}$. This includes both variable splitting and operator splitting. We call it the Composite Splitting Algorithm (CSA). Motivated by the effective acceleration scheme in FISTA (Beck and Teboulle, 2009b), the proposed CSA is further accelerated with an additional acceleration step. Numerous experiments have been conducted on real MR images to compare the proposed algorithm with previous methods. Experimental results show that it impressively outperforms previous methods for the MR image reconstruction in terms of both reconstruction accuracy and computation complexity.

The remainder of the paper is organized as follows. Section 2.1 briefly reviews the related acceleration algorithm FISTA which motivates our method. In Section 2.2, our new MR image reconstruction methods are proposed to solve problem (1). Numerical experiment results are presented in Section 3. Finally, we provide our conclusions in Section 4.

The conference version of this submission has appeared in MICCAI'10 (Huang et al., 2010). This submission has undergone substantial revisions and offers new contributions in the following aspects:

1. The introduction section is rewritten to provide an extensive review of relevant work and to make our contributions clear. Two important optimization techniques are explained for the motivation purpose. Their convergence complexity is also analyzed.
2. We provide the theoretical proof of the algorithm convergence in the methodology section. It mathematically demonstrates the benefit of the proposed method.
3. The experiment section is substantially extended by adding numerous comparisons, such as new data, CPU time, SNR and sample ratio. The extensive comparisons further demonstrate the superior performance of the proposed method.

2. Methodology

2.1. Related acceleration algorithm

In this section, we briefly review the FISTA in Beck and Teboulle (2009b), since our methods are motivated by it. FISTA considers to minimize the following problem:

$$min\{F(x) \equiv f(x) + g(x), x \in \mathbf{R}^{\mathbf{p}}\} \tag{2}$$

where f is a smooth convex function with Lipschitz constant L_f, and g is a convex function which may be nonsmooth.

ϵ-optimal solution: Suppose x^* is an optimal solution to (2). $x \in \mathbf{R}^p$ is called an ϵ-optimal solution to (2) if $F(x) - F(x^*) \leqslant \epsilon$ holds.
Gradient: $\nabla f(x)$ denotes the gradient of the function f at the point x.
The proximal map: given a continuous convex function $g(x)$ and any scalar $\rho > 0$, the proximal map associated with function g is defined as follows (Beck and Teboulle, 2009b; Beck and Teboulle, 2009a):

$$prox_\rho(g)(x) := \arg\min_u \left\{ g(u) + \frac{1}{2\rho}\|u - x\|^2 \right\} \tag{3}$$

Algorithm 1 outlines the FISTA. It can obtain an ϵ-optimal solution in $\mathcal{O}(1/\sqrt{\epsilon})$ iterations.

Theorem 2.1. (Theorem 4.1 in Beck and Teboulle, 2009b): *Suppose $\{x^k\}$ and $\{r^k\}$ are iteratively obtained by the FISTA, then, we have*

$$F(x^k) - F(x^*) \leqslant \frac{2L_f\|x^0 - x^*\|^2}{(k+1)^2}, \quad \forall x^* \in X_*$$

The efficiency of the FISTA highly depends on being able to quickly solve its second step $x^k = prox_\rho(g)(x_g)$. For simpler regularization problems, it is possible, i.e., the FISTA can rapidly solve the $L1$ regularization problem with cost $\mathcal{O}(p\log(p))$ (Beck and Teboulle, 2009b) (where p is the dimension of x), since the second step $x^k = prox_\rho(\beta\|\Phi x\|_1)(x_g)$ has a close form solution; It can also quickly solve the TV regularization problem, since the step $x^k = prox_\rho(\alpha\|x\|_{TV})(x_g)$ can be computed with cost $\mathcal{O}(p)$ (Beck and Teboulle,

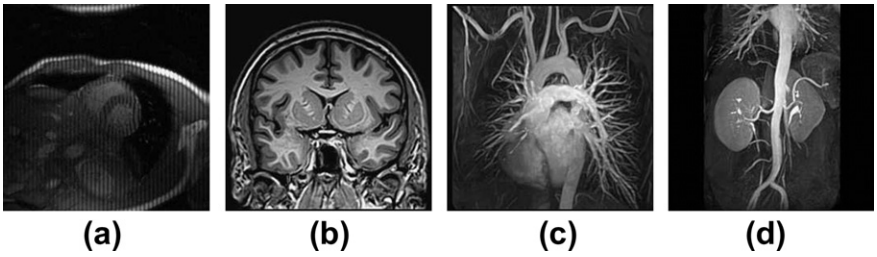

Fig. 1. MR images: (a) cardiac; (b) brain; (c) chest and (d) artery.

2009a). However, the FISTA cannot efficiently solve the composite $L1$ and TV regularization problem (1), since no efficient algorithm exists to solve the step

Algorithm 1. FISTA (Beck and Teboulle, 2009b)

Input: $\rho = 1/L_f$, $r^1 = x^0$, $t^1 = 1$
for $k = 1$ **to** K **do**
  $x_g = r^k - \rho\nabla f(r^k)$
  $x^k = prox_\rho(g)(x_g)$
  $t^{k+1} = \frac{1+\sqrt{1+4(t^k)^2}}{2}$
  $r^{k+1} = x^k + \frac{t^k-1}{t^{k+1}}(x^k - x^{k-1})$
end for

Algorithm 2. CSD

Input: $\rho = 1/L,\ \alpha,\ \beta,\ z_1^0 = z_2^0 = x_g$
for $j = 1$ **to** J **do**
  $x_1 = prox_\rho(2\alpha\|x\|_{TV})(z_1^{j-1})$
  $x_2 = prox_\rho(2\beta\|\Phi x\|_1)(z_2^{j-1})$
  $x^j = (x_1 + x_2)/2$
  $z_1^j = z_1^{j-1} + x^j - x_1$
  $z_2^j = z_2^{j-1} + x^j - x_2$
end for

$$x^k = prox_\rho(\alpha\|x\|_{TV} + \beta\|\Phi x\|_1)(x_g). \tag{4}$$

To solve the problem (1), the key problem is thus to develop an efficient algorithm to solve problem (4). In the following section, we will show that a scheme based on composite splitting techniques can be used to do this.

2.2. CSA and FCSA

From the above introduction, we know that, if we can develop a fast algorithm to solve problem (4), the MR image reconstruction problem can then be efficiently solved by the FISTA, which obtains an ϵ-optimal solution in $\mathcal{O}(1/\sqrt{\epsilon})$ iterations. Actually, problem (4) can be considered as a denoising problem:

$$x^k = \arg\min_x \left\{\frac{1}{2}\|x - x_g\|^2 + \rho\alpha\|x\|_{TV} + \rho\beta\|\Phi x\|_1\right\}. \tag{5}$$

We use composite splitting techniques to solve this problem: (1) splitting variable x into two variables $\{x_i\}_{i=1,2}$; (2) performing operator splitting over each of $\{x_i\}_{i=1,2}$ independently and (3) obtaining the solution x by linear combination of $\{x_i\}_{i=1,2}$. We call it Composite Splitting Denoising (CSD) method, which is outlined in Algorithm 2. Its validity is guaranteed by the following theorem:

Theorem 2.2. *Suppose $\{x^j\}$ the sequence generated by the CSD. Then, x^j will converge to $prox_\rho(\alpha\|x\|_{TV} + \beta\|\Phi x\|_1)(x_g)$, which means that we have $x^j \to prox_\rho(\alpha\|x\|_{TV} + \beta\|\Phi x\|_1)(x_g)$.*

Sketch Proof of The Theorem 2.2:
Consider a more general formulation:

$$\min_{x\in\mathbf{R}^p} F(x) \equiv f(x) + \sum_{i=1}^m g_i(B_i x) \tag{6}$$

where f is the loss function and $\{g_i\}_{i=1,\ldots,m}$ are the prior models, both of which are convex functions; $\{B_i\}_{i=1,\ldots,m}$ are orthogonal matrices.

Proposition 2.1. (Theorem 3.4 in Combettes and Pesquet, 2008): *Let $\mathcal{H}$ be a real Hilbert space, and let $g = \sum_{i=1}^m g_i$ in $\Gamma_0(\mathcal{H})$ such that dom $g_i \cap$ dom $g_j \neq \emptyset$. Let $r \in \mathcal{H}$ and $\{x_j\}$ be generated by the Algorithm 3. Then, x_j will converge to prox(g)(r).*

The detailed proof for this proposition can be found in Combettes and Pesquet (2008) and Combettes (2009).

Algorithm 3. (Algorithm 3.1 in Combettes and Pesquet, 2008)

Input: ρ,$\{z_i\}_{i=1,\ldots,m} = r$, $\{w_i\}_{i=1,\ldots,m} = 1/m$,
for $j = 1$ **to** J **do**
  for $i = 1$ **to** m **do**
    $p_{i,j} = prox_\rho(g_i/w_i)(z_j)$
  end for
  $p_j = \sum_{i=1}^m w_i p_{i,j}$
  $q^{j+1} = z_j + q_j - x_j$
  $\lambda_j \in [0,2]$
  for $i = 1$ **to** m **do**
    $z_{i,j+1} = z_{i,j+1} + \lambda_j(2p_j - x_j - p_{i,j})$
  end for
  $x_{j+1} = x_j + \lambda_j(p_j - x_j)$
end for

Suppose that $y_i = B_i x, s_i = B_i^T r$ and $h_i(y_i) = m\rho g_i(B_i x)$. Because the operators $\{B_i\}_{i=1,\ldots,m}$ are orthogonal, we can easily obtain that $\frac{1}{2\rho}\|x - r\|^2 = \sum_{i=1}^m \frac{1}{2m\rho}\|y_i - s_i\|^2$. The above problem is transferred to:

$$\hat{y}_i = \arg\min_{y_i} \sum_{i=1}^m \left[\frac{1}{2}\|y_i - s_i\|^2 + h_i(y_i)\right], \quad x = B_i^T y_i, \quad i = 1,\ldots,m \tag{7}$$

Obviously, this problem can be solved by Algorithm 3. According to Proposition 2.1, we know that x will converge to $prox(g)(r)$. Assuming $g_1(x) = \alpha\|x\|_{TV}$, $g_2(x) = \beta\|x\|_1$, $m = 2$, $w_1 = w_2 = 1/2$ and $\lambda_j = 1$, we obtain the proposed CSD algorithm. x will converge to $prox(g)(r)$, where $g = g_1 + g_2 = \alpha\|x\|_{TV} + \beta\|\Phi x\|_1$. □

Combining the CSD with FISTA, a new algorithm FCSA is proposed for MR image reconstruction problem (1). In practice, we

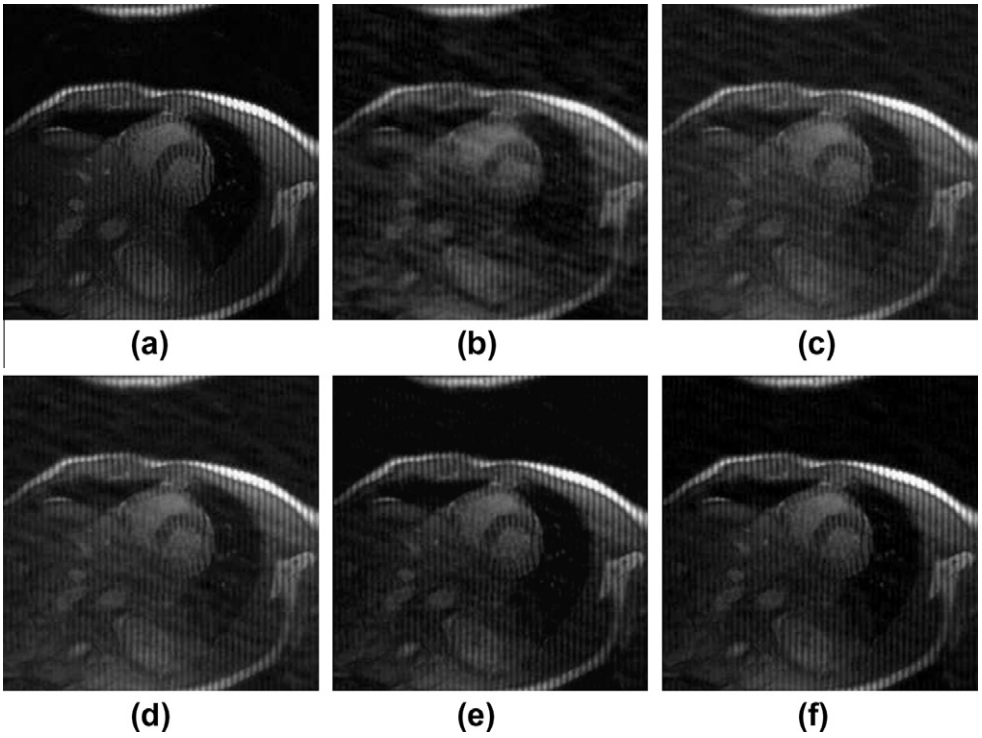

Fig. 2. Cardiac MR image reconstruction from 20% sampling (a) original image; (b–f) are the reconstructed images by the CG (Lustig et al., 2007), TVCMRI (Ma et al., 2008), RecPF (Yang et al., 2010), CSA and FCSA. Their SNR are 9.86, 14.43, 15.20, 16.46 and 17.57 (db). Their CPU time are 2.87, 3.14, 3.07, 2.22 and 2.29 (s).

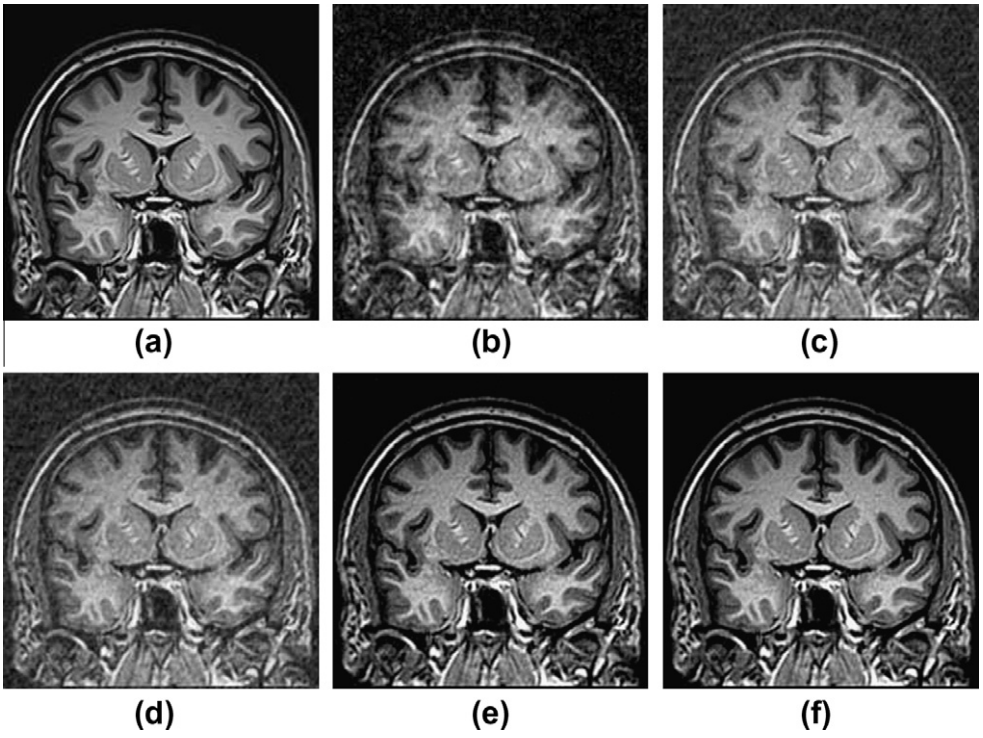

Fig. 3. Brain MR image reconstruction from 20% sampling (a) original image; (b–f) are the reconstructed images by the CG (Lustig et al., 2007), TVCMRI (Ma et al., 2008), RecPF (Yang et al., 2010), CSA and FCSA. Their SNR are 8.71, 12.12, 12.40, 18.68 and 20.35 (db). Their CPU time are 2.75, 3.03, 3.00, 2.22 and 2.20 (s).

found that a small iteration number J in the CSD is enough for the FCSA to obtain good reconstruction results. Especially, it is set as 1 in our algorithm. Numerous experimental results in the next section will show that it is good enough for real MR image reconstruction.

Algorithm 5 outlines the proposed FCSA. In this algorithm, if we remove the acceleration step by setting $t^{k+1} \equiv 1$ in each iteration, we will obtain the Composite Splitting Algorithm (CSA), which is outlined in Algorithm 4. A key feature of the FCSA is its fast convergence performance borrowed from the FISTA. From Theorem 2.1,

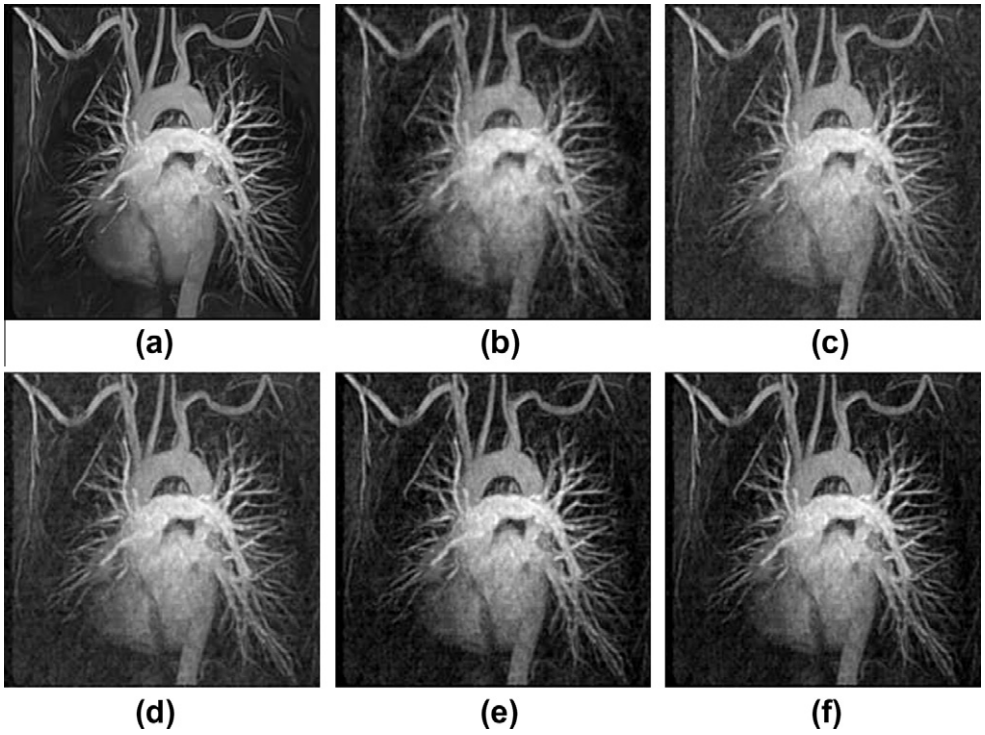

Fig. 4. Chest MR image reconstruction from 20% sampling (a) original image; (b–f) are the reconstructed images by the CG (Lustig et al., 2007), TVCMRI (Ma et al., 2008), RecPF (Yang et al., 2010), CSA and FCSA. Their SNR are 11.80, 15.06, 15.37, 16.53 and 16.07 (db). Their CPU time are 2.95, 3.03, 3.00, 2.29 and 2.234 (s).

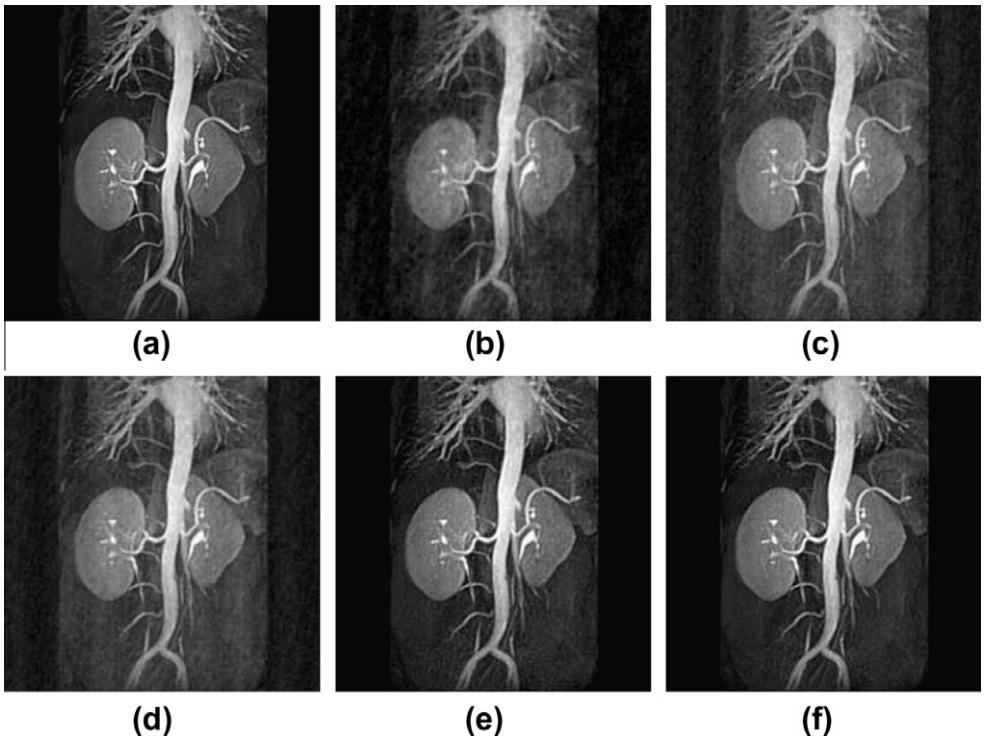

Fig. 5. Artery MR image reconstruction from 20% sampling (a) original image; (b–f) are the reconstructed images by the CG (Lustig et al., 2007), TVCMRI (Ma et al., 2008), RecPF (Yang et al., 2010), CSA and FCSA. Their SNR are 11.73, 15.49, 16.05, 22.27 and 23.70 (db). Their CPU time are 2.78, 3.06, 3.20, 2.22 and 2.20 (s).

we know that the FISTA can obtain an ϵ-optimal solution in $\mathcal{O}(1/\sqrt{\epsilon})$ iterations.

Another key feature of the FCSA is that the cost of each iteration is $\mathcal{O}(p\log(p))$, as confirmed by the following observations. The step 4, 6 and 7 only involve adding vectors or scalars, thus cost only $\mathcal{O}(p)$ or $\mathcal{O}(1)$. In step 1, $\nabla f(r^k = R^T(R\ \ r^k - b))$ since $f(r^k) = \frac{1}{2}\|Rr^k - b\|^2$ in this case. Thus, this step only costs $\mathcal{O}(p\log(p))$. As introduced above, the step $x^k = prox_\rho(2\alpha\|x\|_{TV})(x_g)$ can be computed quickly with cost $\mathcal{O}(p)$ (Beck and Teboulle, 2009a); The step $x^k = prox_\rho(2\beta\|\Phi x\|_1)(x_g)$ has a close form solution and can be

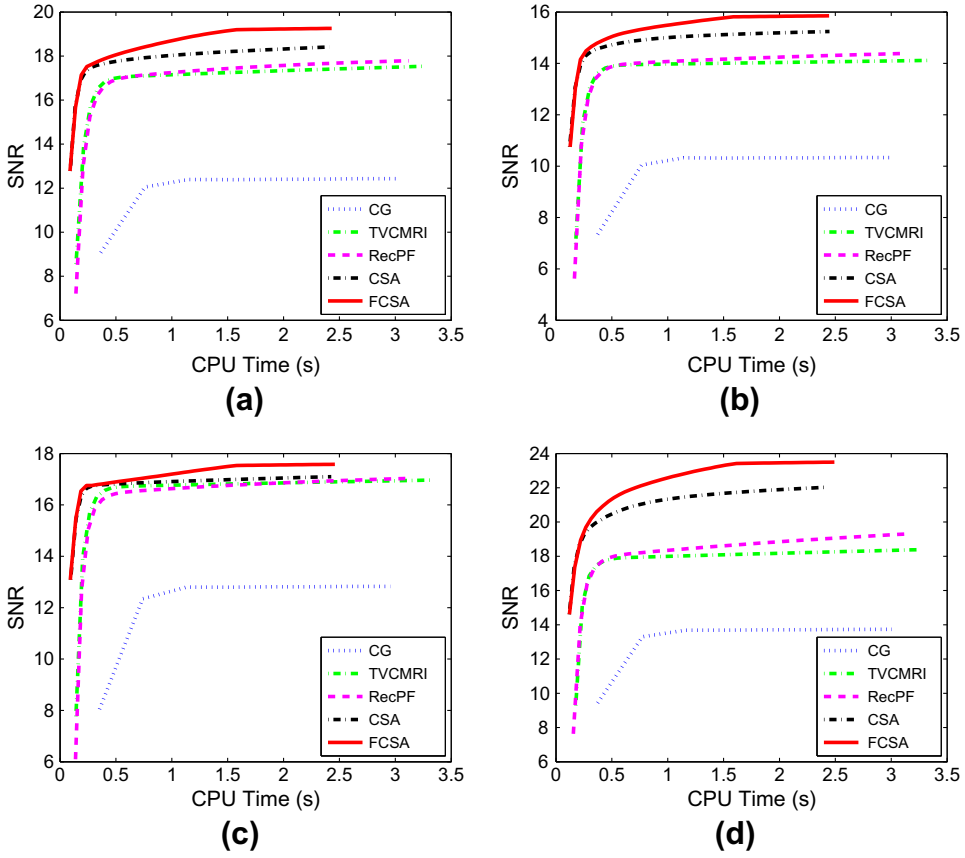

Fig. 6. Performance comparisons (CPU-Time vs. SNR) on different MR images: (a) cardiac image; (b) brain image; (c) chest image and (d) artery image.

Table 1
Comparisons of the SNR (db) over 100 runs.

	CG	TVCMRI	RecPF	CSA	FCSA
Cardiac	12.43 ± 1.53	17.54 ± 0.94	17.79 ± 2.33	18.41 ± 0.73	19.26 ± 0.78
Brain	10.33 ± 1.63	14.11 ± 0.34	14.39 ± 2.17	15.25 ± 0.23	15.86 ± 0.22
Chest	12.83 ± 2.05	16.97 ± 0.32	17.03 ± 2.36	17.10 ± 0.31	17.58 ± 0.32
Artery	13.74 ± 2.28	18.39 ± 0.47	19.30 ± 2.55	22.03 ± 0.18	23.50 ± 0.20

Table 2
Comparisons of the CPU Time (s) over 100 runs.

	CG	TVCMRI	RecPF	CSA	FCSA
Cardiac	2.82 ± 0.16	3.16 ± 0.10	2.97 ± 0.12	2.27 ± 0.08	2.30 ± 0.08
Brain	2.81 ± 0.15	3.12 ± 0.15	2.95 ± 0.10	2.27 ± 0.12	2.31 ± 0.13
Chest	2.79 ± 0.16	3.00 ± 0.11	2.89 ± 0.07	2.21 ± 0.06	2.26 ± 0.07
Artery	2.81 ± 0.17	3.04 ± 0.13	2.94 ± 0.09	2.22 ± 0.07	2.27 ± 0.13

computed with cost $\mathcal{O}(p\log(p))$. In the step $x^k = project(x^k,[l,u])$, the function $x = project(x,[l,u])$ is defined as: (1) $x = x$ if $l \leqslant x \leqslant u$; (2) $x = l$ if $x < u$; and (3) $x = u$ if $x > u$, where $[l,u]$ is the range of x. For example, in the case of MR image reconstruction, we can let $l = 0$ and $u = 255$ for 8-bit gray MR images. This step costs $\mathcal{O}(p)$. Thus, the total cost of each iteration in the FCSA is $\mathcal{O}(p\log(p))$.

With these two key features, the FCSA efficiently solves the MR image reconstruction problem (1) and obtains better reconstruction results in terms of both the reconstruction accuracy and computation complexity. The experimental results in the next section demonstrate its superior performance compared with all previous methods for compressed MR image reconstruction.

Algorithm 4. CSA

Input: $\rho = 1/L$, α, β, $t^1 = 1$ $x^0 = r^1$
for $k = 1$ **to** K **do**
$x_g = r^k - \rho\nabla f(r^k)$
$x_1 = prox_\rho(2\alpha\|x\|_{TV})(x_g)$
$x_2 = prox_\rho(2\beta\|\Phi x\|_1)(x_g)$
$x^k = (x_1 + x_2)/2$
x^k=project $(x^k,[l,u])$
$r^{k+1} = x^k$
endfor

Algorithm 5. FCSA

Input: $\rho = 1/L$, α, β, $t^1 = 1$ $x^0 = r^1$
for $k = 1$ **to** K **do**
$x_g = r^k - \rho\nabla f(r^k)$
$x_1 = prox_\rho(2\alpha\|x\|_{TV})(x_g)$
$x_2 = prox_\rho(2\beta\|\Phi x\|_1)(x_g)$
$x^k = (x_1 + x_2)/2$;
x^k=project $(x^k,[l,u])$
$t^{k+1} = (1 + \sqrt{1 + 4(t^k)^2})/2$
$r^{k+1} = x^k + ((t^k - 1)/t^{k+1})(x^k - x^{k-1})$
end for

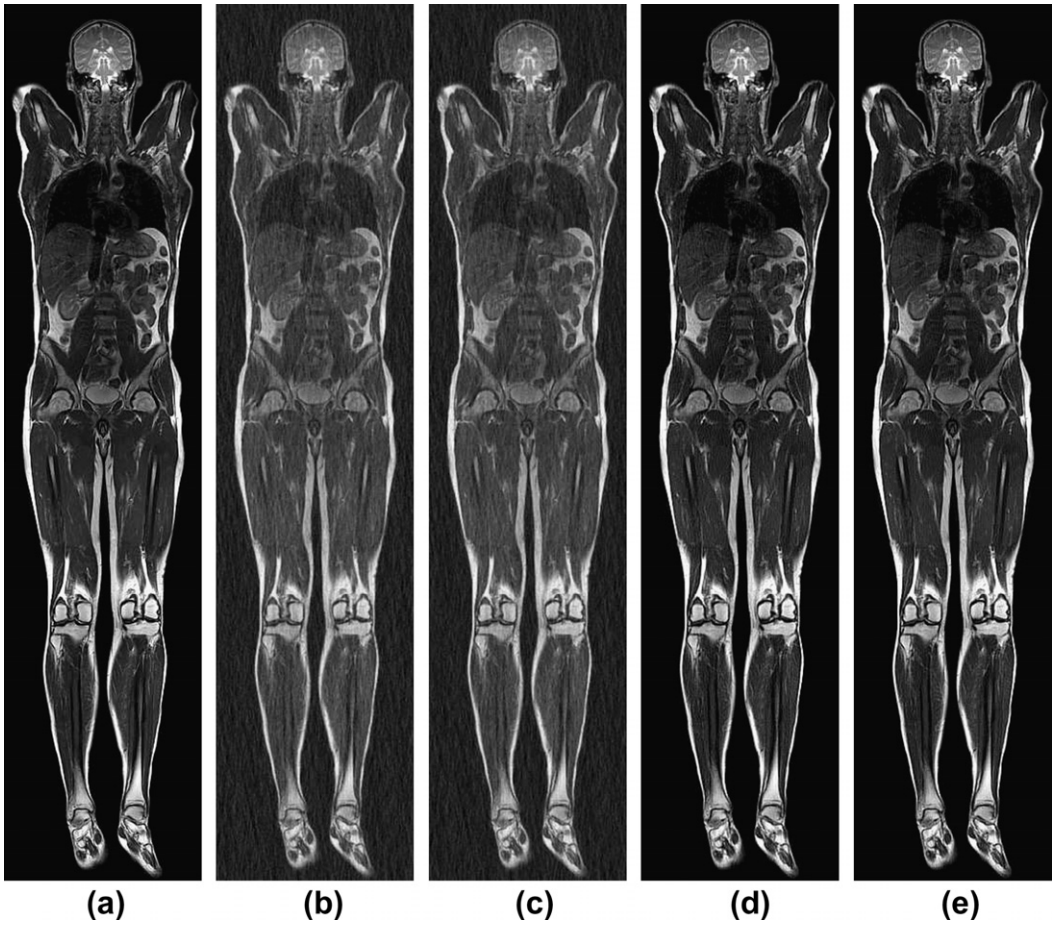

Fig. 7. Full Body MR image reconstruction from 25% sampling (a) original image; (b–e) are the reconstructed images by the TVCMRI (Ma et al., 2008), RecPF (Yang et al., 2010), CSA and FCSA. Their SNR are 12.56, 13.06, 18.21 and 19.45 (db). Their CPU time are 12.57, 11.14, 10.20 and 10.64 (s).

3. Experiments

3.1. Experiment setup

Suppose a MR image x has n pixels, the partial Fourier transform R in problem (1) consists of m rows of a $n \times n$ matrix corresponding to the full 2D discrete Fourier transform. The m selected rows correspond to the acquired b. The sampling ratio is defined as m/n. The scanning duration is shorter if the sampling ratio is smaller. In MR imaging, we have certain freedom to select rows, which correspond to certain frequencies. In the following experiments, we select the corresponding frequencies according to the following manner. In the k-space, we randomly obtain more samples in low frequencies and less samples in higher frequencies. This sampling scheme has been widely used for compressed MR image reconstruction (Lustig et al., 2007; Ma et al., 2008; Yang et al., 2010). Practically, the sampling scheme and speed in MR imaging also depend on the physical and physiological limitations (Lustig et al., 2007).

We implement our CSA and FCSA for problem (1) and apply them on 2D real MR images. The code that was used for the experiment is available for download at the link listed in footnote.[1] All experiments are conducted on a 2.4 GHz PC in Matlab environment. We compare the CSA and FCSA with the classic MR image reconstruction method based on the CG (Lustig et al., 2007). We also compare them with two of the fastest MR image reconstruction methods, TVCMRI[2] (Ma et al., 2008) and RecPF[3] (Yang et al., 2010). For fair comparisons, we download the codes from their websites and carefully follow their experiment setup. For example, the observation measurement b is synthesized as $b = Rx + \mathbf{n}$, where $\mathbf{n}$ is the Gaussian white noise with standard deviation $\sigma = 0.01$. The regularization parameter α and β are set as 0.001 and 0.035. R and b are given as inputs, and x is the unknown target. For quantitative evaluation, the Signal-to-Noise Ratio (SNR) is computed for each reconstruction result. Let x_0 be the original image and x a reconstructed image, the SNR is computed as: $SNR = 10\ \log_{10}(V_s/V_n)$, where V_n is the Mean Square Error between the original image x_0 and the reconstructed image x; $V_s = var(x_0)$ denotes the power level of the original image where $var(x_0)$ denotes the variance of the values in x_0.

3.2. Visual comparisons

We apply all methods on four 2D MR images: cardiac, brain, chest and artery respectively. Fig. 1 shows these images. For convenience, they have the same size of 256×256. The sample ratio is set to be approximately 20%. To perform fair comparisons, all methods run 50 iterations except that the CG runs only eight iterations due to its higher computational complexity.

Figs. 2–5 show the visual comparisons of the reconstructed results by different methods. The FCSA always obtains the best visual

[1] http://paul.rutgers.edu/jzhuang/R_FCSAMRI.htm.

[2] http://www.columbia.edu/sm2756/TVCMRI.htm.

[3] http://www.caam.rice.edu/optimization/L1/RecPF/.

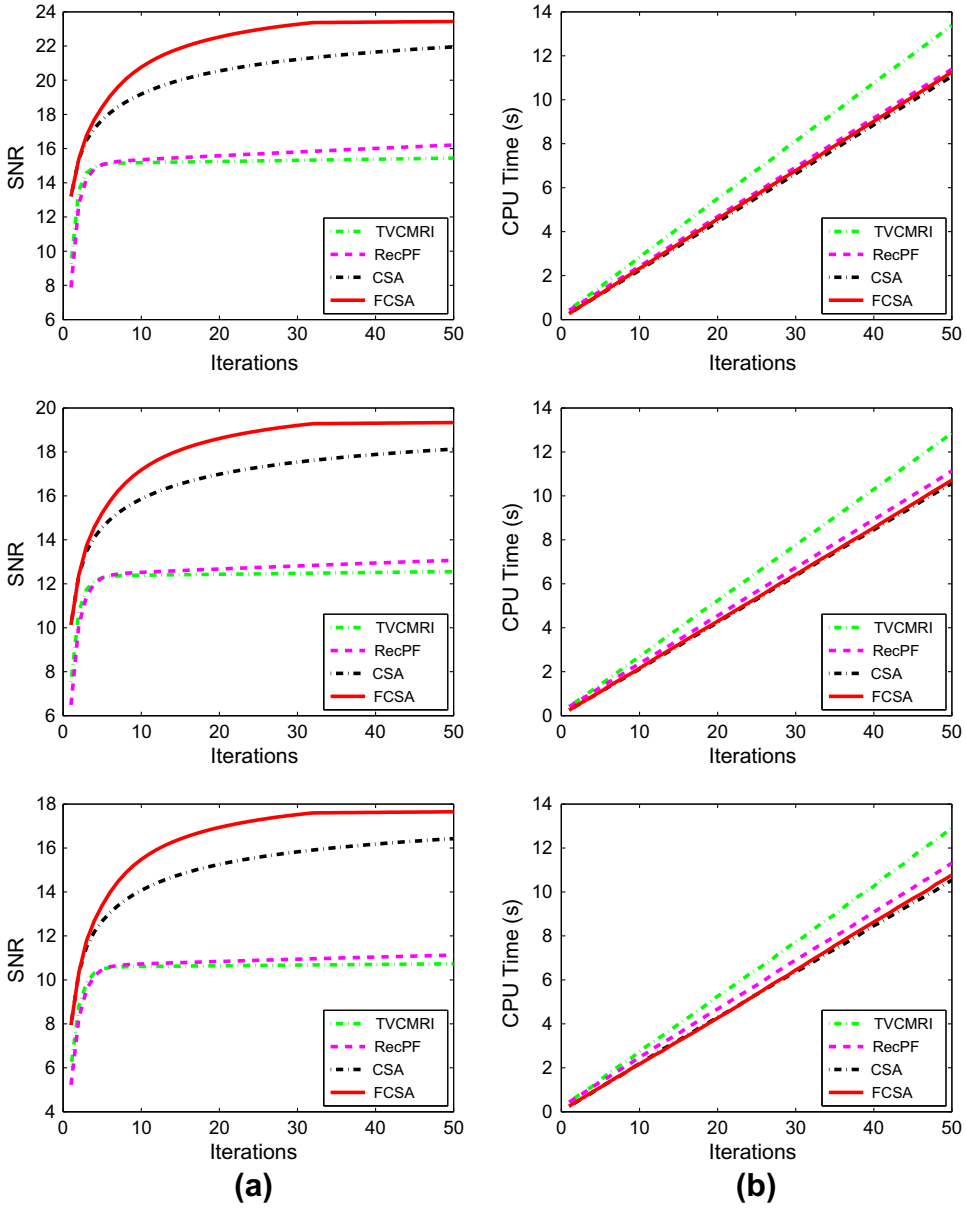

Fig. 8. Performance comparisons on the full body MR image with different sampling ratios. The sample ratios are: (1) 36%; (2) 25% and (3) 20%. The performance: (a) Iterations vs. SNR (db) and (b) iterations vs. CPU time (s).

effects on all MR images in less CPU time. The CSA is always inferior to the FCSA, which shows the effectiveness of acceleration steps in the FCSA for the MR image reconstruction. The classical CG (Lustig et al., 2007) is far worse than others because of its higher cost in each iteration, the RecPF is slightly better than the TVCMRI, which is consistent with observations in Ma et al. (2008) and Yang et al. (2010).

In our experiments, these methods have also been applied on the test images with the sample ratio set to 100%. We observed that all methods obtain almost the same reconstruction results, with SNR 64.8, after sufficient iterations. This was to be expected, since all methods are essentially solving the same formulation "Model (1)".

3.3. CPU time and SNRs

Fig. 6 gives the performance comparisons between different methods in terms of the CPU time over the SNR. Tables 1 and 2 tabulate the SNR and CPU Time by different methods, averaged over 100 runs for each experiment, respectively. The FCSA always obtains the best reconstruction results on all MR images by achieving the highest SNR in less CPU time. The CSA is always inferior to the FCSA, which shows the effectiveness of acceleration steps in the FCSA for the MR image reconstruction. While the classical CG (Lustig et al., 2007) is far worse than others because of its higher cost in each iteration, the RecPF is slightly better than the TVCMRI, which is consistent to observations in Ma et al. (2008) and Yang et al. (2010).

3.4. Sample ratios

To test the efficiency of the proposed method, we further perform experiments on a full body MR image with size of 924×208. Each algorithm runs 50 iterations. Since we have shown that the CG method is far less efficient than other methods, we will not include it in this experiment. The sample ratio is set to be

approximately 25%. To reduce the randomness, we run each experiment 100 times for each parameter setting of each method. The examples of the original and recovered images by different algorithms are shown in Fig. 7. From there, we can observe that the results obtained by the FCSA are not only visibly better, but also superior in terms of both the SNR and CPU time.

To evaluate the reconstruction performance with different sampling ratio, we use sampling ratio 36%, 25% and 20% to obtain the measurement b respectively. Different methods are then used to perform reconstruction. To reduce the randomness, we run each experiments 100 times for each parameter setting of each method. The SNR and CPU time are traced in each iteration for each methods.

Fig. 8 gives the performance comparisons between different methods in terms of the CPU time and SNR when the sampling ratios are 36%, 25% and 20% respectively. The reconstruction results produced by the FCSA are far better than those produced by the CG, TVCMRI and RecPF. The reconstruction performance of the FCSA is always the best in terms of both the reconstruction accuracy and the computational complexity, which further demonstrates the effectiveness and efficiency of the FCSA for the compressed MR image construction.

3.5. Discussion

The experimental results reported above validate the effectiveness and efficiency of the proposed composite splitting algorithms for compressed MR image reconstruction. Our main contributions are:

- We propose an efficient algorithm (FCSA) to reconstruct the compressed MR images. It minimizes a linear combination of three terms corresponding to a least square data fitting, total variation (TV) and L1 norm regularization. The computational complexity of the FCSA is $\mathcal{O}(p\log(p))$ in each iteration (p is the pixel number in reconstructed image). It also has fast convergence properties. It has been shown to significantly outperform the classic CG methods (Lustig et al., 2007) and two state-of-the-art methods (TVCMRI (Ma et al., 2008) and RecPF (Yang et al., 2010)) in terms of both accuracy and complexity.
- The step size in the FCSA is designed according to the inverse of the Lipschitz constant L_f. Actually, using larger values is known to be a way of obtaining faster versions of the algorithm (Wright et al., 2009). Future work will study the combination of this technique with the CSD or FCSA, which is expected to further accelerate the optimization for this kind of problems.
- In this paper, the proposed methods are developed to efficiently solve model (1), which has been addressed by SparseMRI, TVCMRI and RecPF. Therefore, with enough iterations, SparseMRI, TVCMRI and RecPF will obtain the same solution as that obtained by our methods. Since all of them solve the same formulation, they will lead to the same gain in information content. In our future work, we will develop new effective models for compressed MR image reconstruction, which can lead to more information gains.

4. Conclusion

We have proposed an efficient algorithm for the compressed MR image reconstruction. Our work has the following contributions. First, the proposed FCSA can efficiently solve a composite regularization problem including both TV term and L1 norm term, which can be easily extended to other medical image applications. Second, the computational complexity of the FCSA is only $\mathcal{O}(p\log(p))$ in each iteration where p is the pixel number of the reconstructed image. It also has strong convergence properties. These properties make the real compressed MR image reconstruction much more feasible than before. Finally, we conduct numerous experiments to compare different reconstruction methods. Our method is shown to impressively outperform the classical methods and two of the fastest methods so far in terms of both accuracy and complexity.

References

Beck, A., Teboulle, M., 2009a. Fast gradient-based algorithms for constrained total variation image denoising and deblurring problems. IEEE Transaction on Image Processing 18, 2419–2434.

Beck, A., Teboulle, M., 2009b. A fast iterative shrinkage-thresholding algorithm for linear inverse problems. SIAM Journal on Imaging Sciences 2, 183–202.

Candes, E.J., Romberg, J., Tao, T., 2006. Robust uncertainty principles: exact signal reconstruction from highly incomplete frequency information. IEEE Transactions on Information Theory 52, 489–509.

Chartrand, R., 2007. Exact reconstruction of sparse signals via nonconvex minimization. IEEE Signal Processing Letters 14, 707–710.

Chartrand, R., 2009. Fast algorithms for nonconvex compressive sensing: MRI reconstruction from very few data. In: Proceedings of the Sixth IEEE international conference on Symposium on Biomedical Imaging: From Nano to Macro. IEEE Press, pp. 262–265.

Combettes, P.L., 2009. Iterative construction of the resolvent of a sum of maximal monotone operators. Journal of Convex Analysis 16, 727–748.

Combettes, P.L., Pesquet, J.C., 2008. A proximal decomposition method for solving convex variational inverse problems. Inverse Problems 24, 1–27.

Combettes, P.L., Wajs, V.R., 2008. Signal recovery by proximal forward-backward splitting. SIAM Journal on Multiscale Modeling and Simulation 19, 1107–1130.

Donoho, D., 2006. Compressed sensing. IEEE Transactions on Information Theory 52, 1289–1306.

Eckstein, J., Svaiter, B.F., 2009. General projective splitting methods for sums of maximal monotone operators. SIAM Journal on Control Optimization 48, 787–811.

Gabay, D., 1983. Chapter IX applications of the method of multipliers to variational inequalities. Studies in Mathematics and its Applications 15, 299–331.

Gabay, D., Mercier, B., 1976. A dual algorithm for the solution of nonlinear variational problems via finite-element approximations. Computers and Mathematics with Applications 2, 17–40.

Glowinski, R., Le Tallec, P., 1989. Augmented Lagrangian and Operator-Splitting Methods in Nonlinear Mechanics, vol. 9. Society for Industrial Mathematics.

Goldfarb, D., Ma, S., 2009. Fast Multiple Splitting Algorithms for Convex Optimization. Technical Report, Department of IEOR, Columbia University, New York.

He, B.S., Liao, L.Z., Han, D., Yang, H., 2002. A new inexact alternating direction method for monotone variational inequalities. Mathematical Programming 92, 103–118.

He, L., Chang, T.C., Osher, S., Fang, T., Speier, P., 2006. MR image reconstruction by using the iterative refinement method and nonlinear inverse scale space methods. Technical Report UCLA CAM 06-35. <ftp://ftp.math.ucla.edu/pub/camreport/cam06-35.pdf>.

Huang, J., Zhang, S., Metaxas, D., 2010. Efficient MR image reconstruction for compressed MR imaging. In: Proceedings of the 13th International Conference on Medical Image Computing and Computer-Assisted Intervention: Part I. LNCS, vol. 6361. Springer-Verlag, pp. 135–142.

Ji, S., Ye, J., 2009. An accelerated gradient method for trace norm minimization. In: Proceedings of the 26th Annual International Conference on Machine Learning. ACM, pp. 457–464.

Lustig, M., Donoho, D., Pauly, J., 2007. Sparse MRI: the application of compressed sensing for rapid MR imaging. Magnetic Resonance in Medicine 58, 1182–1195.

Ma, S., Yin, W., Zhang, Y., Chakraborty, A., 2008. An efficient algorithm for compressed mr imaging using total variation and wavelets. In: IEEE Conference on Computer Vision and Pattern Recognition, CVPR 2008, pp. 1–8.

Malick, J., Povh, J., Rendl, F., Wiegele, A., 2009. Regularization methods for semidefinite programming. SIAM Journal on Optimization 20, 336–356.

Nesterov, Y.E., 1983. A method for solving the convex programming problem with convergence rate $o(1/k^2)$. Doklady Akademii Nauk SSSR 269, 543–547.

Nesterov, Y.E., 2007. Gradient methods for minimizing composite objective function. Technical Report. <http://www.ecore.beDPs/dp1191313936.pdf>.

Spingarn, J.E., 1983. Partial inverse of a monotone operator. Applied Mathematics and Optimization 10, 247–265.

Trzasko, J., Manduca, A., Borisch, E., 2009. Highly undersampled magnetic resonance image reconstruction via homotopic l0-minimization. IEEE Transactions on Medical Imaging 28, 106–121.

Tseng, P., 1991. Applications of a splitting algorithm to decomposition in convex programming and variational inequalities. SIAM Journal on Control and Optimization 29, 119–138.

Tseng, P., 2000. A modified forward-backward splitting method for maximal monotone mappings. SIAM Journal on Control and Optimization 38, 431–446.

Wang, Y., Yang, J., Yin, W., Zhang, Y., 2008. A new alternating minimization algorithm for total variation image reconstruction. SIAM Journal on Imaging Sciences 1, 248–272.

Wright, S., Nowak, R., Figueiredo, M., 2009. Sparse reconstruction by separable approximation. IEEE Transactions on Signal Processing 57, 2479–2493.

Yang, J., Zhang, Y., Yin, W., 2010. A fast alternating direction method for TVL1-L2 signal reconstruction from partial fourier data. IEEE Journal of Selected Topics in Signal Processing 4, 288–297.

Ye, J., Tak, S., Han, Y., Park, H., 2007. Projection reconstruction MR imaging using focuss. Magnetic Resonance in Medicine 57, 764–775.